The largest extinct volant bird Pelagornis could not meet the energetic demands of skimming

ROYAL SOCIETY OPEN SCIENCE

royalsocietypublishing.org/journal/rsos

Research

Cite this article: Hellyer-Price O, Venditti C, Humphries S. 2026 The largest extinct volant bird *Pelagornis* could not meet the energetic demands of skimming. *R. Soc. Open Sci.* **13**: 251840.
https://doi.org/10.1098/rsos.251840

Received: 23 September 2025
Accepted: 13 November 2025

Subject Category:
Organismal and evolutionary biology

Subject Areas:
biomechanics, palaeontology, ecology

Keywords:
aerodynamics, avian flight, biomechanics, feeding behaviour, *Pelagornis*

Author for correspondence:
Stuart Humphries
e-mail: shumphries@lincoln.ac.uk

Supplementary material is available online at https://doi.org/10.6084/m9.figshare.c.8284774.

THE ROYAL SOCIETY PUBLISHING

The largest extinct volant bird *Pelagornis* could not meet the energetic demands of skimming

Olivia Hellyer-Price[1], Chris Venditti[2] and Stuart Humphries[3]

[1]Département de Biologie, Université PSL, Paris, France
[2]School of Biological Sciences, University of Reading, Reading, Berkshire, UK
[3]Research and Enterprise, University of Lincoln, Lincoln, UK

CV, 0000-0002-6776-2355; SH, 0000-0001-9766-6404

The fossil record is one of our only direct insights into the lives of extinct species. In recent years, the development of biomechanical and aerodynamic models has allowed us to ask specific questions that the fossil records alone cannot answer. *Pelagornis* was a Palaeocene marine bird characterized by a large bill with pseudo-teeth, which has generated debate about the way it may have fed. Here, we assess the idea that *Pelagornis* could have fed by skimming, a feeding behaviour seen almost exclusively in modern skimmers, *Rynchops* (Aves). Using biomechanical models and morphological measurements of the bills of two *Pelagornis* species, *Pelagornis chilensis* and *Pelagornis sandersi*, we show that *Pelagornis* could not have met the energetic requirements of skim-feeding. Additionally, we show that *Pelagornis* could not have overcome the drag induced by picking prey from the surface of the water, shedding doubt on the possibility that *Pelagornis* could have fed from the water's surface. Our results refute the hypothesis that *Pelagornis* could skim-feed and illustrate how biomechanical models can be used to infer ecological interactions of extinct species.

1. Introduction

The fossil record is one of our only insights into the ecologies, lifestyles and evolutionary history of extinct taxa. Comparisons of morphological features in fossilized extinct and extant species have allowed many conclusions to be drawn on how extinct species lived. However, physical comparisons alone can often only reveal a partial picture. The use of biomechanical models

raises the intriguing prospects of uncovering the lifestyles of extinct species in greater detail; such models have already been applied to assessing locomotion [1–5] and feeding mechanics [6–9] of extinct taxa.

Pelagornis is a genus of the extinct marine bird family Pelagornithidae from the Palaeogene [10,11] and exhibits one of the largest wingspans thought to have existed in flighted birds, estimated to be up to 6 m [10,12]. Pelagornithidae are also characterized by the possession of a unique dentary of bony pseudo-teeth [10,13]. It is this unique characteristic, which first raised questions about their ecology, specifically their diet and feeding behaviours [13,14]. It is thought that *Pelagornis* fed on fish and soft-bodied invertebrates [13,15]; however, the mechanism by which *Pelagornis* captured its prey is uncertain, leading to a number of hypotheses. It has been suggested that *Pelagornis* pseudo-teeth could have been for nest raiding or kleptoparasitism [12]. Alternatively, and more similar to close relatives like Procellariformes, *Pelagornis* could have taken prey from the water's surface [16,17], using its hooked maxilla [13] and size-varied pseudo-teeth to grasp prey [18]. In a similar thinking, several studies have postulated that *Pelagornis* could have fed by skimming [10,19–21], supported by the presence of an intraramal joint allowing greater kinesis of the lower mandible [19,22].

Skimming is a feeding mechanism where the lower mandible is partially submerged in the water during flight [16,23,24], seen almost exclusively in extant species belonging to the genus *Rynchops*, the skimmers. Although skimming-like behaviours have been recorded in terns and some gulls, it is uncommon [25,26]. The skimmer bill is highly adapted to their unique feeding behaviour, with the lower mandible being markedly longer than the upper mandible and compressing into a vertical blade [16,24] with riblet structures along the bill to reduce drag [27]. In comparison, the *Pelagornis* bill shows no evidence of such lateral compressions, and a relatively blunt bill tip brings into question its capability of skimming-like behaviours; however, no biomechanical study has ever tested the validity of the skimming-foraging behaviours in *Pelagornis*.

Developments in the use of biomechanical models for the interpretation of ecological interactions of extinct species provide us with an opportunity to test the idea that *Pelagornis* was a skimming feeder. As previously demonstrated in pterosaurs [9], hydrodynamic and aerodynamic theory paired with morphological measurements can be used to estimate the effect that drag from skimming can have on the flight of a species. Here, we use methods from [9] to test if two species of *Pelagornis*, *Pelagornis chilensis* and *Pelagornis sandersi* could overcome the energetic demands of skimming. We estimate the resulting drag on the bill caused by skimming, then scale the estimated power required for flight by this drag. This gives us an estimate of the metabolic power required for flight while skimming, P_{met}. While flying close to the ground or the surface of the water, birds experience the wing-in-ground effect, where circulating air currents become trapped between the surface and the wings. Such an effect will occur while skimming and can reduce the energetic burden of flight. We estimate the effects of this phenomenon on P_{met} and scale the power accordingly.

We compare the results *of Pelagornis* to those of a modern-day skimmer species, *Rynchops niger cinerascens*, a subspecies of black skimmer, to illustrate the difference in skimming ability. Ksepka speculated whether *Pelagornis* would have been able to feed in a similar manner to the largest volant extant birds, such as the albatross, while noting that it was debatable *Pelagornis* would have been able to take off from the sea surface [12]. Other extant birds can pick food objects off the surface of the water without having to land, such as a frigatebird, or just under the surface of the water while remaining in flight, sometimes referred to as air or contact dipping [28]. However, there is yet to be a model that describes such behaviour in birds. To give an indication of *Pelagornis* ability to sustain flight while capturing food from the surface, we use our skimming model to assess *Pelagornis*'s flight ability with reduced proportions of the bill breaking the water, 10% and 5%. We compare *Pelagornis*'s ability with that of two pelagic bird species under the same 10% or 5% submersion model, the black-footed albatross (*Phoebastria nigripes*) and the magnificent frigatebird (*Fregata magnificens*).

2. Material and methods

2.1. Data collection

Mass estimated for *P. chilensis* was taken from [19], and from [12] for *P. sandersi*; both references used the scaling relationship between mass and femoral circumference. Wingspan for *P. sandersi* was likewise taken from [12], taking the mid-point from an estimated range. Wingspan for *P. chilensis* was taken from [19]. Published photographs of the jaw were taken from [19] for *P. chilensis* and [12] for

P. sandersi. Jaw measurements were taken from published photographs of specimens for each species using the software ImageJ [29]. Multiple measurements were taken for the total jaw length, tip width (the length of the tip of the mandible measured from one lateral side to the other), chord length (measured on the ventral side of the mandible from one lateral side to the other) and bill thickness at 19%, 10% and 5% for the jaw length (measured on the lateral side of the jaw, dorsal to ventral edge). Data for modern birds were collected from a variety of sources: *Rynchops* wing and bill data from [9], *F. magnificens* and *P. nigripes* wing data taken from [30], *F. magnificens* bill measurements were made of photographs from [31] using the software ImageJ [29], and *P. nigripes* bill measurements were taken from three-dimensional scans available through MorphoSource (https://www.morphosource.org/ [OUVC]:[WitmerLab]:[10 905], ark:/87602 /m4/M78049), measured with MeshLab [32]. All data can be found in the electronic supplementary material, data S1.

2.2. Drag modelling

Below, we outline the model describing drag created by skimming, estimates of flight power parameters and influence of the wing-in-ground effect. Simple models can adequately illuminate the basic and fundamental principles of locomotion [33,34], while we acknowledge that more complex models exist (e.g. accounting for wing kinematics [35]), which require additional assumptions that are difficult, if not impossible, to formulate with data from extinct organisms.

To model the drag on the bill induced by skimming, we follow methods by Humphries *et al.* [9] adapted from Hoerner [36], modelling the bills as surface-piercing struts. Throughout, the mandible was assumed to be inclined at a 45 degree angle in a downwards direction [23].

We estimated the total drag acting on the submerged bill (D_{tot}) by summing three drag components associated with skimming: bill profile drag (D_{proB}), spray drag (D_{spray}) and drag owing to ventilation (D_{vent}). We follow the assumptions of Humphries *et al.* [9] that the effects of wave drag are negligible and thus can be ignored:

$$D_{\text{tot}} = D_{\text{proB}} + D_{\text{spray}} + D_{\text{vent}}, \tag{2.1}$$

D_{proB} represents both the friction and pressure drag acting on the bill and is found using the equation,

$$D_{\text{proB}} = 0.5\rho_{\text{w}} V^2 S_{\text{bill}} \text{Cd}_{\text{proB}}, \tag{2.2}$$

where ρ_{w} is the density of water, V is the velocity of the bill, S_{bill} is the frontal projected area of the bill and Cd_{proB} is the coefficient of bill profile drag. Cd_{proB}, and thus D_{proB}, is dependent on the Reynolds number (Re), a ratio of inertial to viscous forces used to predict fluid flow patterns [37]. We describe the Re dependence of Cd_{proB} of the bill using the following equation except when $10^4 \leq Re \leq 10^7$, where the coefficient of the bill profile drag (Cd_{proB}) is approximately constant [38]. We follow the assumption of Humphries *et al.* [9] that *Rynchops* bill should be modelled on a thin plate in laminar flow.

$$\text{Cd}_{\text{proB}} = 2C_{\text{fL}}\left(\frac{c}{t_{\text{mid}}}\right), \tag{2.3}$$

where C_{fL} is the coefficient of skin friction drag for laminar flow, $1.328/Re^{1/2}$, c is the chord and t_{mid} is the thickness of the bill at the midpoint between the tip and water surface.

Spray drag is induced when the bill breaks the surface of the water and is dependent on Froude number (Fr), a measure of the ratio of inertial and gravitational forces [9]. Again, we follow Humphries *et al.* [9] assumption that when $Fr < 3$, the effects of spray drag are negligible ($Fr < 3$, D_{spray} is assumed 0) and are only estimated when $Fr \geq 3$

$$D_{\text{spray}} = 0.5\rho_{\text{w}} V^2 t_{\text{int}}^2 \text{Cd}_{\text{spray}}, \tag{2.4}$$

where t_{int} is the thickness of the bill at the water surface interface, being the thickness of the tip of the bill, and Cd_{spray} is the coefficient of spray drag, which at $Fr \geq 3$ is constant at the order 0.24 [9].

Finally, drag owing to ventilation is associated with the drag created by areas or pockets of negative pressure behind the moving object.

$$D_{\text{vent}} = 0.5p_{\text{w}} V^2 S_{\text{bill}} \text{Cd}_{\text{vent}}, \tag{2.5}$$

where Cd_{vent} is the coefficient of ventilation drag and is found using the following equation,

$$\mathrm{Cd}_{\mathrm{vent}} = \frac{gd}{V^2}, \tag{2.6}$$

where g is the acceleration due to gravity (9.81 m s^{-2}), and d is the depth at which the tip of the bill penetrates the water; this is measured at 5%, 10% and 19%.

The above drag estimations are modelled on a flat plate under laminar flow (a hydrodynamic model), such to describe the hydrodynamic drag experienced by the skimmers [9]. Drag estimations were also modelled on a NACA 0012 aerofoil with a blunt leading edge (an aerodynamic model), more in line with the blunt nature of the *Pelagornis* bill, which differs only in the calculation of the coefficient of bill profile drags calculation. $\mathrm{Cd}_{\mathrm{proB}}$ in both contexts is dependent on the *Re* number, when $Re \leq 10^5$

$$\mathrm{Cd}_{\mathrm{proB}} = 2C_{\mathrm{fL}}\left(\frac{c}{t_{\mathrm{mid}}}\right) + 2C_{\mathrm{fL}} + \left(\frac{t_{\mathrm{mid}}}{c}\right). \tag{2.7}$$

When $Re > 10^5$

$$\mathrm{Cd}_{\mathrm{proB}} = 1 + 2\left(\frac{t_{\mathrm{mid}}}{c}\right) + 2C_{\mathrm{fT}}\left(\frac{c}{t_{\mathrm{mid}}}\right)60\left(\frac{t_{\mathrm{mid}}}{c}\right)^4, \tag{2.8}$$

where C_{fT} is the skin friction drag for turbulent flow:

$$C_{\mathrm{fT}} = \frac{1}{(5.5 - 3.46\,\mathrm{Log}(Re)^2)}. \tag{2.9}$$

2.3. Flight modelling

We estimate the metabolic power required for powered flight (P_{met}) using a flight model developed by [37].

$$P_{\mathrm{met}} = 1.1\left(\left(\frac{P_{\mathrm{mech}}}{E_{\mathrm{FM}}}\right) + P_{\mathrm{BMR}}\right). \tag{2.10}$$

P_{met} is a product of the total mechanical power expended (P_{mech}), the flight muscle efficiency (E_{FM}), and basal metabolic rate (P_{BMR}). E_{FM} represents the metabolic power consumed by the flight muscles (an efficiency term related to the mechanical cost) and here is set as a commonly used constant of 0.23 [39]. We use a scaling relationship with mass to estimate P_{BMR}, $P_{\mathrm{BMR}} = 3.277\ \mathrm{M}^{0.624}$ [1,40]. The total power requirement is a product of three parameters; profile power (P_{pro}; a multiple of the absolute minimum power), parasitic power (P_{par}; power to support the weight of the body) and induced power (P_{ind}; power to overcome the drag of the body) [37].

$$P_{\mathrm{mech}} = P_{\mathrm{par}} + P_{\mathrm{ind}} + P_{\mathrm{pro}}, \tag{2.11}$$

where;

$$P_{\mathrm{par}} = \frac{\rho V^3 S \mathrm{Cd}_{\mathrm{body}}}{2}, \tag{2.12}$$

where ρ is the air density (1.23 kg m^{-3}), V is the velocity, S is the frontal projected area calculated from a scaling relationship with mass ($S = 0.00813\ \mathrm{M}^{0.666}$) [39] and $\mathrm{Cd}_{\mathrm{body}}$ is the body drag coefficient. We use methods by [2] who calculate $\mathrm{Cd}_{\mathrm{body}}$ as a product of the lift surface (W_{area}/S),

$$\mathrm{Cd}_{\mathrm{body}} = 0.01\left(\frac{W_{\mathrm{area}}}{S}\right), \tag{2.13}$$

where W_{area} is the wing area, estimated from the wingspan (W^2 aspect ratio^{-1}) according to [37]. We report results using an aspect ratio of 11, similar to that of modern albatross [41]. Alternative higher aspect ratios were tested with minimal impact and no effect on the qualitative results of the study. The induced power (P_{ind}) is a product of the weight of the bird (Mg, mass given the acceleration due to gravity), wingspan (W), air density (ρ) and the induced power scaling factor ($k = 1.2$). P_{ind} has been found to be underestimated in birds given the use of a helicopter model, which estimates P_{ind} based on the air flowing over a wing disc (actuator disc) [37]. However, it is impractical, and in extinct species, it is impossible to calculate the induced power directly, such as in a wind tunnel. Therefore, the actuator disc estimate of induced power is used as a minimum baseline and scaled by a factor, k [37].

$$P_{\text{ind}} = \frac{2k(\text{Mg})^2}{\pi W^2 V \rho}. \tag{2.14}$$

Finally, the profile power is a product of the profile power constant (8.4) [37], the wing aspect ratio (AR) and the absolute minimum power (P_{am}):

$$P_{\text{pro}} = \left(\frac{8.4}{\text{AR}}\right) P_{\text{am}}, \tag{2.15}$$

$$\text{AR} = \frac{W^2}{W_{\text{area}}}, \tag{2.16}$$

where P_{am} is found as the sum of the parasitic and induced power at their minimum power speed (V_{mp}), the speed at which the power required is the lowest [42].

2.4. Modelling wing-in-ground effect

When flying close to the ground, the wings experience an 'in-ground effect' because of interactions between air movement and the water or land surface, which alters the aerodynamic properties of the wing, significantly affecting flight performance [43]. We account for this by correcting the total mechanical power (P_{mech}) for the ground effect by incorporating the coefficients δ, the reduction in drag owing to ground effect [9], and D_{ge}, a factor to describe the increase in circulation of air around the wing owing to ground effect [9,43]:

$$P_{\text{ge}} = \frac{(P_{\text{mech}} D_{\text{ge}})}{\delta}, \tag{2.17}$$

where δ is the relative drag, and D_{ge} is the total drag corrected for the in-ground effect [9], a product of the relative circulation (γ) and scaled velocity (v):

$$\delta = \frac{1}{2v^2} + \frac{v^2}{2}, \tag{2.18}$$

$$D_{\text{ge}} = \frac{\gamma^2(1-\sigma)}{2} + \frac{v^2}{2}, \tag{2.19}$$

where;

$$\gamma = \frac{\left(V - \left(V^2 - 2\tau r_{\text{D}}\right)^{\frac{1}{2}}\right)}{\tau r_{\text{D}}}, \tag{2.20}$$

$$v = \frac{V}{V_{\text{mp}}}, \tag{2.21}$$

where V is the velocity, V_{mp} is the minimum power speed, the velocity at which the power cost is minimized [9,42], σ is the induced drag of the in-ground effect and τ is a circulation factor owing to the in-ground effect. τ and σ are derived graphically as a function of height/semi-wingspan ($\beta = h/b$) [43]. r_{D} is the minimum drag-to-weight ratio.

$$r_{\text{D}} = 2\left(\frac{\text{Cd}_{\text{body}}}{\pi \text{AR}}\right)^{\frac{1}{2}}, \tag{2.22}$$

where Cd_{body} and AR are derived using equations (2.13) and (2.16).

P_{ge} in equation (2.17) is used to scale the power output of flight, which provides us with a new total mechanical power output (P_{mech}) that accounts for the in-ground effect. We can then use this P_{mech} in equation (2.10) to estimate the metabolic power required for powered flight with the in-ground effect.

3. Results

Our models do not incorporate the pseudo-teeth of *Pelagornis*; however, we can assume that the presence of teeth would cause increased drag on the bill, disrupting any laminar flow of the water around the bill and creating additional energetic costs. Previous work has indicated that a

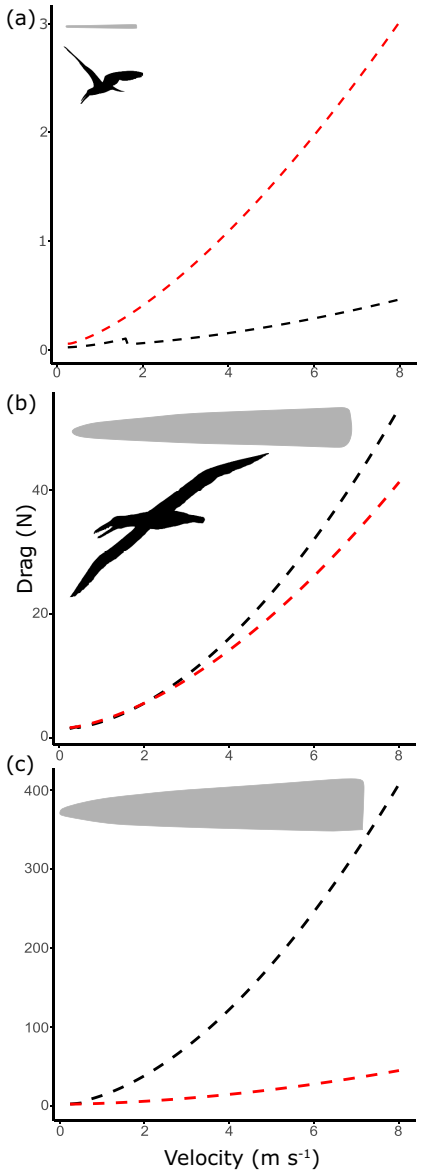

Figure 1. Measurements of the total drag induced by skimming on the bills (grey silhouettes) of *Rynchops* (a), *Pelagornis chilensis* (b), and *Pelagornis sandersi* (c) over a range of velocities. Dashed lines are drag estimates from fluid dynamic models, the black is an aerodynamic model and the red is a hydrodynamic model (thin-plate approximations). We see a shift in the aerodynamic modelled drag (black dashed line) in *Rynchops* owing to a shift in the Reynolds number regime within our model (see §3). Grey silhouettes represent scaled transverse images of the bill to give a comparison of size and shape.

hydrodynamic model presents a good fit to the empirical data for skimmers [9], in line with this work, we report drag values for *Rynchops* from hydrodynamic drag models. Estimates of the total drag on the bill induced by the immersion of the lower bill while skimming for *Rynchops* showed an increase of 0.18 N, increasing from 0.04 to 0.22 N (black line in figure 1a) between the speeds of 1.8–6.8 m s^{-1}, a range benchmarked against empirical measurements in a prior study [9]. However, it is paramount to note that we expect the range of optimal speeds for *Pelagornis* to differ from *Rynchops*, given the size difference between the species (electronic supplementary material, data). In comparison, *P. chilensis* experiences an 8-fold increase in drag from 4.85 to 39.86 N (figure 1b, black line) while *P. sandersi* experienced a 9-fold increase from 32.05 to 305.89 N (figure 1c, black line), most likely owing to *P. sandersi*'s larger and wider bill.

We estimated the total metabolic power consumption of flight (P_{met}), including the drag induced by skimming with the bill submerged at 19%, which is observed in the skimming of *Rynchops* [9]. *Rynchops* was found to have a minimum P_{met} of 14.5 W during skimming (figure 2, black triangle), a 1.4 × increase from 10.3 W during flight away from the water surface (figure 2, black circle). The minimum

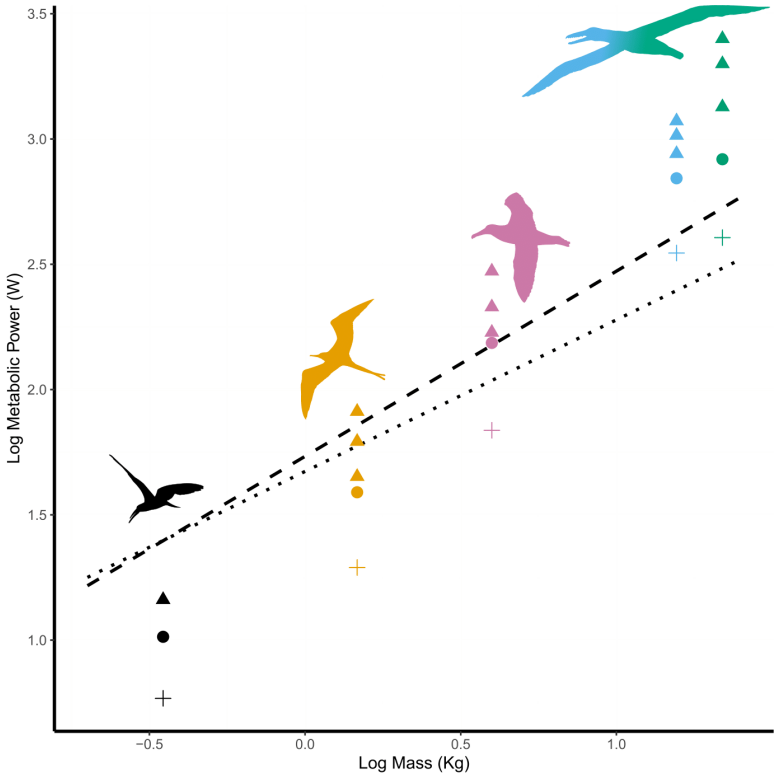

Figure 2. Estimated metabolic costs (minimum P_{met}) of five bird species against mass; black points, *Rynchops*; orange points, *Fregata magnificens*; pink points, *Phoebastria nigripes*; blue points, *Pelagornis chilensis*; green points, *Pelagornis sandersi*. Filled circular points describe the metabolic cost in flapping flight and crosses the metabolic cost during flapping flight experiencing a wing-in-ground effect both without any bill submersion. Triangle points describe the metabolic costs of flight with the bill at 19%, 10% and 5% submerged in the water. Dashed black line indicates the estimated maximum available metabolic power (54.144 $M^{0.739}$) [44], dotted black line the theoretical maximum available power (47.126 $M^{0.605}$) [44].

P_{met} of *P. chilensis* was estimated to double from 551.0 to 1032.9 W with 19% of the bill submerged (figure 2, blue points) and in *P. sandersi* this was shown to triple from 830.3 to 2512.9 W (figure 2, green points). *Pelagornis* could have performed different feeding mechanics at various bill submersion proportions, as reported for albatrosses [45] and frigatebirds [46], which are known to take prey from the water surface, submerging less of their bill than the 19% seen in *Rynchops* (figure 2, orange and pink). We therefore estimate the minimum P_{met} when the proportion of the bill submerged is at 10% and 5%, to test if *Pelagornis* could sustain flight with a reduced proportion of its bill submerged. We see a drop in the minimum P_{met} for both *Pelagornis* species when the submerged proportion of the bill is reduced to 10% (1180.0 W for *P. chilenesis*, 1995.2 W for *P. sandersi*) and a reduction again when this is reduced to 5% (873.3 W for *P. chilensis*, 1342.4 W for *P. sandersi*).

Rynchops, both in skimming and in normal flight, sits well below the theoretical and estimated maximum available metabolic power (figure 2, dashed and dotted lines), being the maximum amount of power a bird can output [44]. Sitting below these lines signifies that the bird can meet the amount of power expended during flight, sitting above suggests the bird cannot meet the energetic demand of the task. Similarly, compared to *Rynchops*, but at reduced bill submersion proportions, frigatebirds fall below this threshold, indicating their ability to meet the energetic needs to remain in flight while having a proportion of their bill submerged. Frigatebirds are known to pluck food items from the surface of the water, not needing to submerge more than a small proportion of the bill [46]. Albatross with a bill submersion of 5% sit just above this threshold (figure 2, pink triangle). Albatross are known to land on the sea surface to catch fish and to consume their prey [47], taking off from the surface of the water afterwards. Both *P. chilensis* and *P. sandersi* sit above this maximum metabolic power estimation, even after reducing the proportion of the bill submerged. The only occurrence of these species sitting below the estimated maximum metabolic power (figure 2, dashed line) is during normal flapping flight without submersion of the bill and including wing-in-ground effects, which reduce the energetic burden of flight [43]. We use measurements of masses derived from femur circumferences, and median values of estimated wingspans in our estimation of *Pelagornis* flight ability (see §). To

assess if changes to these measurements would allow *Pelagornis* to fall further below these maximum power thresholds, we estimated the power required for powered flight, using ranges reported for both mass and wingspan (electronic supplementary material, data S1). We find that even in cases where the smallest mass estimate and largest wingspan estimate were used, qualitatively our results remain the same (electronic supplementary material, figure S1).

4. Discussion

Drag on the bill of *Pelagornis* while skimming is orders of magnitude greater than that experienced by *Rynchops*, even without the consideration of *Pelagornis'* pseudo-teeth, which would induce a considerable amount of additional drag. We demonstrate here that neither *P. chilensis* nor *P. sandersi* would have been able to meet the energetic requirements to overcome the drag induced by skimming at a variety of bill submersion depths. The evidence presented here refutes the hypothesis that *Pelagornis* could have foraged by skimming [19,20] and also draws doubt on whether *Pelagornis* could take prey from the water's surface.

There remains to be an aerodynamic model that can describe the behaviour of capturing prey from the water surface. However, during such behaviours, the bill must be submerged partially in the water during flight, which we can assess here using our skimming model to provide an indication of whether *Pelagornis* could take prey from the water surface. When assessing species known to collect prey from the surface, the magnificent frigatebird, we find that the frigatebird is capable of submerging 5% and 10% of its bill within its energetic capabilities. Species, such as the albatross, alternatively are known to dive in the water after their prey or hunt while sitting on the surface [48]. We find that for albatross to sustain flight while having their bill submerged, even as little as 5%, would probably be very energetically costly, if not above its energetic capabilities. Our model illustrates that even at a greatly reduced submersion of the bill (5%), *Pelagornis* would not have been able to meet the energetic requirements to sustain flight, casting doubt on *Pelagornis* ability to capture prey from the water's surface on the wing.

It is possible for birds to exceed their maximum metabolic power limit through short periods of anaerobic metabolism to overcome energetically expensive flight scenarios, such as short-distance low-speed flight, such as in take-offs and some feeding manoeuvres. Physiological adaptations (such as in the composition of muscle fibres) can increase a bird's ability to overcome its maximum metabolic power limit, if only for a brief time [44]. Behavioural adaptations, such as perching-hunting seen in bats [49], allow flying animals adequate time to recover from large expenditures of energy. Whether *Pelagornis* possessed the ability to overcome its metabolic power limit either through physiological or behavioural adaptation is difficult to determine from the fossil evidence alone, but it is a possibility, nonetheless. However, the power required for *Pelagornis* to successfully skim-forage sits substantially above the maximum metabolic line (figure 2—logged axes), meaning any physiological mechanism would have to meet a considerably large power threshold.

Alternative feeding hypotheses have been discussed, such as kleptoparasitism, also seen in frigate birds [46], and nest raiding as a potential feeding mechanism for *Pelagornis* [12]. Both would be aided by its pseudo-teeth, which in a skimming form of feeding would cause a substantial amount of additional drag. Alternatively, *Pelagornis* could have taken on a more predatory role, such as that of the great skuas, which readily and aggressively attack other birds such as puffins and gannets [50,51].

The powered flight capabilities of *Pelagornis* have been previously assessed, with doubt shed on whether *Pelagornis* would have been able to meet the energetic demands of sustained powered flapping flight [12]. In concordance with prior findings, we find that it was likely *Pelagornis* would not have been able to meet the energetic requirements of sustained powered flight (figure 2, blue and green filled circles). Our findings suggest that *Pelagornis* may have been able to execute a form of flapping flight close to the surface with assistance from the wing-in-ground effect, although energetically costly (figure 2, blue and green crosses), only just sitting beneath the line of maximum available metabolic power.

Pelagornis belongs to a unique extinct clade of toothed birds [52], a feature lost in modern taxa. We reconfirm here the potential of biomechanical models in making inferences about species of the past where the only insight into their lifestyles is the fossil record. Such methods present an opportunity to broaden our understanding of ecologies in extinct species that could be applied to a range of other avian or flying taxa.

Ethics. This work did not require ethical approval from a human subject or animal welfare committee.
Data accessibility. Data are available in the electronic supplementary material online [53].
Declaration of AI use. We have not used AI-assisted technologies in creating this article.
Authors' contributions. O.H.-P.: conceptualization, data curation, formal analysis, investigation, methodology, project administration, visualization, writing—original draft, writing—review and editing; C.V.: conceptualization, formal analysis, funding acquisition, methodology, project administration, resources, validation, writing—original draft, writing—review and editing; S.H.: conceptualization, methodology, software, supervision, validation, writing—original draft, writing—review and editing. All authors gave final approval for publication and agreed to be held accountable for the work performed therein.
Conflict of interest declaration. We declare we have no competing interests.
Funding. This work was supported by the Leverhulme Trust Research Project Grant RL-2019-012 and a University of Reading PhD studentship.

References

1. Venditti C, Baker J, Benton MJ, Meade A, Humphries S. 2020 150 million years of sustained increase in pterosaur flight efficiency. *Nature* **587**, 83–86. (doi:10.1038/s41586-020-2858-8)
2. Serrano FJ, Chiappe LM. 2017 Aerodynamic modelling of a Cretaceous bird reveals thermal soaring capabilities during early avian evolution. *J. R. Soc. Interface* **14**, 20170182. (doi:10.1098/rsif.2017.0182)
3. Dyke G, de Kat R, Palmer C, van der Kindere J, Naish D, Ganapathisubramani B. 2013 Aerodynamic performance of the feathered dinosaur *Microraptor* and the evolution of feathered flight. *Nat. Commun*. **4**, 1. (doi:10.1038/ncomms3489)
4. Sane SP. 2003 The aerodynamics of insect flight. *J. Exp. Biol*. **206**, 23. (doi:10.1242/jeb.00663)
5. Hedenström A, Johansson LC. 2015 Bat flight: aerodynamics, kinematics and flight morphology. *J. Exp. Biol*. **218**, 5. (doi:10.1242/jeb.031203)
6. Sakamoto M. 2010 Jaw biomechanics and the evolution of biting performance in theropod dinosaurs. *Proc. R. Soc. B* **277**, 3327–3333. (doi:10.1098/rspb.2010.0794)
7. Habegger ML, Motta PJ, Huber DR, Dean MN. 2012 Feeding biomechanics and theoretical calculations of bite force in bull sharks (*Carcharhinus leucas*) during ontogeny. *Zoology* **115**, 354–364. (doi:10.1016/j.zool.2012.04.007)
8. Santana SE. 2016 Quantifying the effect of gape and morphology on bite force: biomechanical modelling and *in vivo* measurements in bats. *Funct. Ecol*. **30**, 557–565. (doi:10.1111/1365-2435.12522)
9. Humphries S, Bonser RHC, Witton MP, Martill DM. 2007 Did pterosaurs feed by skimming? Physical modelling and anatomical evaluation of an unusual feeding method. *PLoS Biol*. **5**, e204. (doi:10.1371/journal.pbio.0050204)
10. Kloess PA, Poust AW, Stidham TA. 2020 Earliest fossils of giant-sized bony-toothed birds (*Aves: Pelagornithidae*) from the Eocene of Seymour Island, Antarctica. *Sci. Rep*. **10**. (doi:10.1038/s41598-020-75248-6)
11. Cannell A, Degrange FJ. 2025 Into thin air: the loss of the Pliocene giant volant birds. *Evol. Earth* **3**, 100055. (doi:10.1016/j.eve.2024.100055)
12. Ksepka DT. 2014 Flight performance of the largest volant bird. *Proc. Natl Acad. Sci. USA* **111**, 10624–10629. (doi:10.1073/pnas.1320297111)
13. Mayr G. 2009 *Paleogene fossil birds*. Berlin: Springer Science & Business Media. (doi:10.1007/978-3-540-89628-9)
14. Zusi RL, Warheit KI, Campbell K. 1992 On the evolution of intraramal mandibular joints in pseudodontorns (Aves: Odontopterygia).' See no.36 (1992) - Papers in avian paleontology honoring Pierce Brodkorb - Biodiversity Heritage Library (ed. KE Campbell). In *Proceedings of the II. International Symposium of the Society of Avian Paleontology and Evolution*, Natural History Museum of Los Angeles County 28 - 30 September 1988. LA, USA: Natural History Museum.
15. Olson SL. 1985 The fossil record of birds. In *Avian biology* (eds DS Farner, JR King, KC Parkes), pp. 79–238. New York, NY: Academic Press. (doi:10.1016/b978-0-12-249408-6.50011-x)
16. Zusi RL. 1962 *Structural adaptations of the head and neck in the black skimmer:* Rynchops nigra *Linnaeus*. Cambridge, MA: Nuttall Ornithological Club. (doi:10.5962/bhl.title.155041)
17. Warheit KI. 1992 A review of the fossil seabirds from the Tertiary of the North Pacific: plate tectonics, paleoceanography, and faunal change. *Paleobiology* **18**, 401–424. (doi:10.1017/s0094837300010976)
18. Piro A, Acosta Hospitaleche C. 2024 The rhamphotheca of the Eocene pseudo-toothed birds from Antarctica. *Hist. Biol* **36**, 1745–1753. (doi:10.1080/08912963.2023.2230584)
19. Mayr G, RUBILAR-Rogers D. 2010 Osteology of a new giant bony-toothed bird from the Miocene of Chile, with a revision of the taxonomy of Neogene Pelagornithidae. *J. Vertebr. Paleontol*. **30**, 1313–1330. (doi:10.1080/02724634.2010.501465)
20. Mayr G. 2011 Cenozoic mystery birds – on the phylogenetic affinities of bony-toothed birds (*Pelagornithidae*). *Zool. Scr*. **40**, 448–467. (doi:10.1111/j.1463-6409.2011.00484.x)
21. Mayr G, De Pietri VL, Love L, Mannering A, Scofield RP. 2021 Oldest, smallest and phylogenetically most basal pelagornithid, from the early Paleocene of New Zealand, sheds light on the evolutionary history of the largest flying birds. *Pap. Palaeontol*. **7**, 217–233. (doi:10.1002/spp2.1284)
22. Naish D. 2014 The fossil record of bird behaviour. *J. Zool*. **292**, 268–280. (doi:10.1111/jzo.12113)

23. Withers PC, Timko PL. 1977 The significance of ground effect to the aerodynamic cost of flight and energetics of the black skimmer (*Rhyncops nigra*). *J. Exp. Biol.* **70**, 13–26. (doi:10.1242/jeb.70.1.13)
24. Martin GR, Mcneil R, Rojas LM. 2007 Vision and the foraging technique of skimmers (*Rynchopidae*). *Ibis* **149**, 750–757. (doi:10.1111/j.1474-919x.2007.00706.x)
25. Tomkins IT. 1951 Method of feeding of the black skimmer, *Rynchops nigra*. *Auk* **68**, 236–239. (doi:10.2307/4081193)
26. Grace JW. 1980 Cleptoparasitism by ring-billed gulls of wintering waterfowl. *Wilson Bull* **92**, 246–248.
27. Martin S, Bhushan B. 2016 Discovery of riblets in a bird beak (*Rynchops*) for low fluid drag. *Phil. Trans. R. Soc. A* **374**, 20160134. (doi:10.1098/rsta.2016.0134)
28. Ashmole NP, Ashmole MJ. 1967 Comparative feeding ecology of sea birds of a tropical oceanic island. *Bull. Peabody Mus. Nat. Hist.* **40**, 1–131.
29. Schneider CA, Rasband WS, Eliceiri KW. 2012 NIH Image to ImageJ: 25 years of image analysis. *Nat. Methods* **9**, 671–675. (doi:10.1038/nmeth.2089)
30. Taylor G, Thomas A. 2014 *Evolutionary biomechanics: selection, phylogeny and constraint*. Oxford, UK: Oxford University Press.
31. Carlos CJ, Alvarenga JG, Mazzochi MS. 2017 Osteology of the feeding apparatus of magnificent frigatebird *Fregata magnificens* and brown booby *Sula leucogaster* (Aves: Suliformes). *Papéis Avulsos De Zool*. **57**, 265–274. (doi:10.11606/0031-1049.2017.57.20)
32. Cignoni P, Callieri M, Corsini M, Dellepiane M, Ganovelli F, Ranzuglia G. 2008 MeshLab: an Open-Source Mesh Processing Tool (eds V Scarano, R De Chiara, U Erra). In *Eurographics Italian Chapter Conference*. Salerno, Italy: The Eurographics Association. (doi:%2010.2312/LocalChapterEvents/ItalChap/ItalianChapConf2008/129-136)
33. Alexander RM. 2005 Models and the scaling of energy costs for locomotion. *J. Exp. Biol*. **208**, 9. (doi:10.1242/jeb.01484)
34. Alexander RM. 1997 Simple models of human locomotion. *J. Theor. Med*. **1**, 129–135. (doi:10.1080/10273669708833013)
35. Heerenbrink MK, Johansson LC, Hedenström A. 2015 Power of the wingbeat: modelling the effects of flapping wings in vertebrate flight. *Proc. R. Soc. A* **471**, 20140952. (doi:10.1098/rspa.2014.0952)
36. Hoerner SF. 1965 *Fluid-dynamic drag: theoretical, experimental, and statistical information*. Bakersfield, CA: Hoerner Fluid Dynamics.
37. Pennycuick CJ. 2008 *Modelling the flying bird*. Amsterdam, The Netherlands: Elsevier.
38. Sheldahl RE, Klimas PC. 1981 Aerodynamic characteristics of seven symmetrical airfoil sections through 180-degree angle of attack for use in aerodynamic analysis of vertical axis wind turbines (doi:10.2172/6548367)
39. Pennycuick CJ. 1989 *Bird flight performance: a practical calculation manual*. Oxford, UK: Oxford University Press.
40. Londoño GA, Chappell MA, Castañeda M del R, Jankowski JE, Robinson SK. 2015 Basal metabolism in tropical birds: latitude, altitude, and the 'pace of life'. *Funct. Ecol.* **29**, 338–346. (doi:10.1111/1365-2435.12348)
41. Stempeck A, Hassanalian M, Abdelkefi A. 2018 Aerodynamic performance of albatross-inspired wing shape for marine unmanned air vehicles. In *2018 Aviation Technology, Integration, and Operations Conference*, Atlanta, Georgia. Reston, Virginia. (doi:10.2514/6.2018-3899). https://arc.aiaa.org/doi/book/10.2514/MATI018.
42. Norberg RA. 1981 Optimal flight speed in birds when feeding young. *J. Anim. Ecol*. **50**, 7. (doi:10.2307/4068)
43. Rayner J. 1991 On the aerodynamics of animal flight in ground effect. *Phil. Trans. R. Soc. Lond. B* **334**, 119–128. (doi:10.1098/rstb.1991.0101)
44. Marden JH. 1994 From damselflies to pterosaurs: how burst and sustainable flight performance scale with size. *Am. J. Physiol*. **266**, R1077–84. (doi:10.1152/ajpregu.1994.266.4.R1077)
45. Prince PA, Huin N, Weimerskirch H. 1994 Diving depths of albatrosses. *Antarct. Sci*. **6**, 353–354. (doi:10.1017/s0954102094000532)
46. Diamond AW, Schreiber EA. 2002 Magnificent Frigatebird (Fregata magnificens), version 1.0. In *Birds of the world* (eds AF Poole, FB Gill). Ithaca, NY, USA: Cornell Lab of Ornithology. (doi:10.2173/bow.magfri.01)
47. Antolos M, Shaffer SA, Weimerskirch H, Tremblay Y, Costa DP. 2017 Foraging Behavior and Energetics of Albatrosses in Contrasting Breeding Environments. *Front. Mar. Sci.* **4**, 2296–7745. (doi:10.3389/fmars.2017.00414)
48. Weimerskirch H, Pinaud D, Pawlowski F, Bost CA. 2007 Does prey capture induce area-restricted search? A fine-scale study using GPS in a marine predator, the wandering albatross. *Am. Nat*. **170**, 734–743. (doi:10.1086/522059)
49. Voigt CC, Schuller BM, Greif S, Siemers BM. 2010 Perch-hunting in insectivorous Rhinolophus bats is related to the high energy costs of manoeuvring in flight. *J. Comp. Physiol. B* **180**, 1079–1088. (doi:10.1007/s00360-010-0466-x)
50. Andersson M. 1976 Predation and kleptoparasitism by skuas in a Shetland seabird colony. *Ibis* **118**, 208–217. (doi:10.1111/j.1474-919x.1976.tb03066.x)
51. Bayes JC, Dawson MJ, Potts GR. 1964 The food and feeding behaviour of the great skua in the Faroes. *Bird Study* **11**, 272–279. (doi:10.1080/00063656409476077)
52. Louchart A, Sire JY, Mourer-Chauviré C, Geraads D, Viriot L, de Buffrénil V. 2013 Structure and growth pattern of pseudoteeth in *Pelagornis mauretanicus* (Aves, Odontopterygiformes, Pelagornithidae). *PLoS ONE* **8**, e80372. (doi:10.1371/journal.pone.0080372)
53. Hellyer-Price O, Venditti C, Humphries S. 2026 Supplementary material from: The largest extinct volant bird Pelagornis could not meet the energetic demands of skimming. FigShare. (doi:10.6084/m9.figshare.c.8284774)